Prony's method as a tool for power system identification in Smart Grids

Sjur Føyen
Dept. of Electric Power Eng.
NTNU
Trondheim, Norway
sjur.foyen@gmail.com

Mads-Emil Kvammen
Dept. of Electric Power Eng.
NTNU
Trondheim, Norway
mekvammen@gmail.com

Olav Bjarte Fosso
Dept. of Electric Power Eng.
NTNU
Trondheim, Norway
olav.fosso@ntnu.no

***Abstract*—This paper investigates the theory, intuition and performance of two known implementations of Prony's method. Such methods are useful for identifying the individual modes of a system without constructing a component-based model. In the Smart Grid, Prony Analysis has been widely used on post-disturbance ring-down measurements, which have been increasingly available with the extensive deployment of PMU's. Both methods decompose the signal into decaying sinusoidals, and estimate the frequency, damping, amplitude and phase of each modal component. The first method is based on the original Prony's method, whilst the second method is based on the thought that the system can be viewed as a digital synthesis problem where the system has the properties of an infinite impulse response filter. Both methods employ EMD-based pre-filtering. Additionally, a cluster based approach is proposed for circumventing the issue of determining model order, so that the true modes of the estimation can be distinguished from the trivial modes.**

***Index Terms*—Prony Analysis, model order, modal analysis, signal processing, linear prediction model, linear time-invariant systems, clustering, empirical mode decomposition**

I. Introduction

Prony's method with it's variations are ways for extracting modal information from a signal. The signal is modeled as a sum of damped, complex exponentials - or equivalently - decaying sinusoidals. The goal is to determine the frequency, damping, phase and amplitude of these components. The first description of such a method is not new, in fact, it was first discovered by Gaspard de Prony in the 18th' century [1]. Several of the involved process tasks are demanding, like rooting a high order polynomial and performing linear least-square estimation, although with present computing power these have become trivial matters. Prony Analysis (PA) for power system ringdown analysis was initiated in 1990 by J.F. Hauer [2]. Since then, significant research has been made in order to tackle low-damped small-signal oscillations in the power system. High frequency measurement equipment like Phasor Measurement Units, have been instrumental to the implementation of real-time observation and control of the Smart Grid. Huang *et al.* [3] gives a thorough presentation of the motivation for measurement-based mode tracking and control, and presents a tool for aiding operating personnel.

Different versions of Prony have recently been implemented and used for practical, industrial purposes in the power system sector, as seen in [4] and [5]. Prony's method can be classified as a linear modal estimation technique, and is used on ringdown signals where the modal components are observable. There are other methods in this category, as the Matrix Pencil method and the Eigensystem Realization Algorithm (ERA) [6]. In industry as well as academia, non-linear methods for modal estimation are emerging. The Variable Projection method is one example of this [6].

The motivation for this paper is to address some of the major issues with Prony analysis as a measurement-based modal estimation technique. Empirical mode decomposition (EMD) is used as a robust pre-filtering technique to remove high frequency noise. Clustering methods for all modes found by running Prony for multiple model orders, are used to avoid the need for specifying this in advance. The latter reduces the need for *a priori* knowledge of the signal, and more importantly, increases the trustworthiness of the results.

As most documentation available rely on heavy experience from signal analysis theory, this paper aims at providing a pedagogical introduction to the underlying concepts of each method. They will be described and demonstrated as general signal analysis tools, yet the paper is partly influenced by the Smart Grid perspective. The first method is here referred to as **Original Prony** (abbreviated PA_O), as it is the same theory as initially used by Gaspard de Prony. The second is named **Prony Filter** (PA_F), for it is implemented from the perspective of digital filter theory [7]. However, both arrive at the same end-point, the modal decomposition information of the signal. Note that both methods are implemented as off-line, block-processing methods. This is to reduce the comprehensiveness of the theory. For real-time applications, the reader is referred to the improved recursive Prony algorithm proposed in [8].

Three steps are made for testing the two methods. The first is to create synthetic signals, so that the desired outcome is known. Secondly, time-domain simulations are

done for a small power system model, where the desired information is partially known through linearization of the component-based model. The final step is to test with PMU data from real world Smart Grid event.

II. Theory

A. Discretization

Although there are different ways of conducting a Prony analysis, they all rely on important concepts in the field of signal analysis. In order to fully understand any implementation of Prony, it is essential to be familiar with these concepts. The starting point is to determine the desired model as a Linear Time-Invariant (LTI) system. Such a system can be characterised entirely by a single function called the system's impulse response. LTI systems are subject to several mathematical concepts laid out in [9]. An example of a time-continuous LTI model is given below.

$$c_2\frac{\delta^2 y(t)}{\delta t^2}+c_1\frac{\delta y(t)}{\delta t}=d_2\frac{\delta^2 x(t)}{\delta t^2}+d_1\frac{\delta x(t)}{\delta t}+d_0 x(t) \quad (1)$$

where $y(t)$ = response (output), $x(t)$ = excitation (input) and c, d = constant coefficients.

This describes the system as a time-continuous model. However, the measurement values are obtained as samples at discrete time points. Thus, the model must be described with finite differences, that is, with discrete equations. This conversion is of course not necessary if the physical phenomena actually is discrete. However, as many models are time-continuous, this theory serves as a connection between the time-continuous model, and the sinusoid information obtained through the discrete analysis of Prony.

$$\begin{aligned} y(t) &= y[n] \\ \frac{\delta^p y(t)}{\delta t^p} &= \frac{\nabla^p y[n]}{h^p}+O(h) \end{aligned} \quad (2)$$

where O(h) is leading error of order h and

$$\frac{\nabla^p y[n]}{h^p} \propto y[n]-y[n-1]-\ldots-y[n-p]$$

where (2) shows the relationship between derivatives and backward finite differences [10]. Rewriting (1) as an approximated discrete system yields:

$$a_0 y[n]+a_1 y[n-1]+a_2 y[n-2]=b_0 x[n]+b_1 x[n-1]+b_2 x[n-2] \quad (3)$$

where a and b are coefficients different from - but related to - c and d in (1).

Rearranging, and generalizing to p previous values for y, and q previous values for x gives the general difference equation shown in (4).

The estimation of a_i and b_i is the desired information for deriving the modal decomposition of the signal. From this point on, the derivation of the two methods will differ.

$$y[n]=-\sum_{i=1}^{p} a_i y[n-i]+\sum_{i=0}^{q} b_i x[n-i] \quad (4)$$

B. Original Prony

PA_O assumes zero input to the system, which eliminates the b_i-terms. This difference equation represents a Linear Prediction Model (LPM). Having N number of samples, and choosing a model order p, the LPM can be extended to (5) by stating that the difference equation should be satisfied for the previous $(N-p)$ measurements:

$$\underbrace{-\begin{bmatrix} y[N-1] \\ y[N-2] \\ \vdots \\ y[p] \end{bmatrix}}_{=\mathbf{b}} = \underbrace{\begin{bmatrix} y[N-2] & y[N-3] & \cdots & y[N-p-1] \\ y[N-3] & y[N-4] & \cdots & y[N-p-2] \\ \vdots & \vdots & \ddots & \vdots \\ y[p-1] & y[p-2] & \cdots & y[0] \end{bmatrix}}_{=\mathbf{A}} \cdot \begin{bmatrix} a_1 \\ \vdots \\ a_p \end{bmatrix} \quad (5)$$

This is an over-determined system for $N > 2p$, with $(N-p)$ rows and p columns. For solving this system, the linear least-square approximation method is used, yielding an estimation of the **a**-coefficients that will describe a model close to the measured values. This method is intuitively described in [11, Ch. 4.3].

The next step is to connect these predictor coefficients to the modal decomposition. This is done through the Z-transform. It is shown in [12] that they form the characteristic equation in (6):

$$1+a_1 z^{-1}+\ldots+a_P z^{-p}=0 \quad (6)$$

The polynomial is factorized in order to obtain the roots of the polynomial (e.g. by using the freely available numpy.roots in python).

These roots are closely linked to the eigenvalues of the modal decomposition in the following manner:

$$\lambda_n = f_{samp}\ln\zeta_n \quad (7)$$

Where f_{samp} is the sampling frequency of the input signal and ζ_n is the corresponding polynomial root. From the eigenvalues, the frequencies f and damping ratios η are found:

$$f_n=\frac{|Im(\lambda_n)|}{2\cdot\pi} \qquad \eta_n=\frac{Re(\lambda_n)}{|\lambda_n|} \quad (8)$$

The amplitude and phase of the modal components are estimated by another least-squares approximation. Extending equation (9) to all measurement values, results in equation (10), as stated in [13].

C. Prony filter

In this Prony variation, the perspective is slightly different. The system is assumed to be a Linear Time-Invariant system (LTI-system) with the properties of an Infinite Impulse Response filter (IIR-filter) [14, chap. 10].

$$y[k]=\sum_{i=1}^{p} C_i \zeta_i^k, \quad k=0,1,...,N-1 \tag{9}$$

Where $C_i=\frac{1}{2}A_i e^{\pm j\phi_i}$

$$\begin{bmatrix} y[0] \\ y[1] \\ \vdots \\ y[N-1] \end{bmatrix} = \begin{bmatrix} \zeta_1^0 & \cdots & \zeta_p^0 \\ \zeta_1^1 & \cdots & \zeta_p^1 \\ \vdots & \ddots & \vdots \\ \zeta_1^{N-1} & \cdots & \zeta_P^{N-1} \end{bmatrix} \cdot \underbrace{\begin{bmatrix} C_1 \\ C_2 \\ \vdots \\ C_p \end{bmatrix}}_{=\mathbf{c}} \tag{10}$$

Modelling the system as an IIR-filter means that an impulse is assumed to excite the system at time $t = t_0$ through the system transfer function, which results in a time-response that is possible to measure. This can be viewed as a digital synthesis problem, which means that the desired information is an approximated transfer function that models the system response as close as possible.

By utilizing the Z-transform and its timeshift operator on the difference equation in (4), the transfer function of the system can be obtained.

$$\begin{aligned} Z\{y[n]\} &= -a_1 Y(z)z^{-1} - \ldots - a_p Y(z)z^{-p} + b_0 X(z) + \ldots + b_q X(z)z^{-q} \\ &\Downarrow \\ Y(z) &= -Y(z)\left(a_1 z^{-1} + \ldots + a_p z^{-p}\right) + X(z)\left(b_0 z^0 + \ldots + b_q z^{-q}\right) \\ &\Downarrow \\ Y(z)\left(1 + a_1 z^{-1} + \ldots + a_p z^{-p}\right) &= X(z)\left(b_0 + \ldots + b_q z^{-q}\right) \\ &\Downarrow \\ \frac{Y(z)}{X(z)} = H(z) &= \frac{b_0 + b_1 z^{-1} + \ldots + b_q z^{-q}}{1 + a_1 z^{-1} + \ldots + a_p z^{-p}} \end{aligned} \tag{11}$$

The main difference in the two methods can be seen already. PA_O assumes all input to be zero - eliminating the terms with **b**-coefficients from the difference equation. In PA_F all input is zero, *except* $x[0]$ which is equal to 1, resulting in q zeros in the transfer function. An important assumption in PA_F is that the resulting IIR filter is causal. This is ensured if the order of the denominator p is greater that the order of the nominator q [14, p. 145], and that the signal prior to $t = t[0]$ is assumed to be zero. To ensure this, and to avoid unnecessary computations without much improvement of the result, the q-order is set to $p-1$.

It can be noted that the coefficients are strictly real numbers. From the general difference equation, inserting $x[0]=1$ and remembering that b_n equals zero for $n>q$, the equation system shown in equation (12) can be obtained.

Firstly, the least square solution for the **a**-coefficients in equation (12) is found for $n=q+1$ to $n=N$, similar to equation (5). Note that given the same p-order, PA_F utilizes $p-q-1$ more equations than PA_O for determining the **a**-coefficients.

$$\begin{aligned} n=0&: \; b_0 - y[0] = 0 \\ n=1&: \; b_1 - y[1] - a_1 y[0] = 0 \\ &\vdots \\ n=q&: \; b_q - y[q] - a_1 y[q-1] - \ldots - a_q y[0] = 0 \\ n=q+1&: \; -y[q+1] - a_1 y[q] - \ldots - a_{q+1} y[0] = 0 \\ &\vdots \\ n=p&: \; -y[p] - a_1 y[p-1] - \ldots - a_p y[0] = 0 \\ &\vdots \\ n=N&: \; -y[N] - a_1 y[N-1] - \ldots - a_p y[N-p] = 0 \end{aligned} \tag{12}$$

The next step is to solve for the **b**-coefficients by using equation (12) for $n=0$ to $n=q$. There is no need for least-square approximation as this system has only one unique solution.

The eigenvalues, and thus frequency and damping, can be found from the roots of the denominator (poles) in equation (11) (similar to PA_O). The very same roots are used in a Laurent series expansion of the transfer function, to find the amplitude and phase of the modal components.

$$H(z)=\frac{R_1}{z^{-1}+\zeta_1}+\ldots+\frac{R_p}{z^{-1}+\zeta_p} \tag{13}$$

Where R_n is the residue connected to the pole ζ_n for n from 1 to p. It is important to remember that the poles appear in complex conjugate pairs in this calculation. The residue is given as a complex value where the amplitude and phase can be found from the absolute value and angle respectively. To find the modes and thus frequency and damping, the poles need to be scaled as shown in equation (7). Lastly, the frequency and damping is found using equation (8).

D. EMD

There exists a variety of solutions to improve PAs robustness under noisy conditions. Kumaresan and Feng [15] propose two different pre-filtering methods to improve PA, one based on a predefined FIR filter and one defining the pre-filter iteratively from the measured data. Pre-filtering using the EMD-technique is also proposed in [16].

In this paper, Empirical Mode Decomposition (EMD) is used as a band pass filter, removing high frequency noise and the signal trend. EMD is a method for nonlinear, non-stationary signal processing that decomposes the signal into a set of Intrinsic Mode Functions (IMFs) [17]. The conditions for an IMF are that its mean value is zero, and that the number of extremas equals the number of zero-crossings (or at most differs by one). The stepwise process to identify IMFs in a measured signal $y(t)$ is:

1) Start with signal y(t) as input
2) Identify extremas
3) Calculate the upper and lower envelope of the signal (e_{up}, e_{down})

4) Find the mean value ($m(t)$) of the upper and lower envelope
5) Extract the difference from the signal: $d(t) = y(t)$ - $m(t)$
6) Repeat step 2-5 with $d(t)$ as input, until it satisfies the conditions of an IMF
7) Set $d(t)$ as an IMF, and subtract it from the input signal. Repeat the process with the residue $r(t)$ as input signal ($r(t) = y(t)$ - $d(t)$)
8) Continue until there are no more extrema present in signal

The EMD output extracts modal components starting with the highest frequency and ending with the residual "trend" of the signal. The hierarchy in the decomposed modes gives the EMD characteristics similar to that of a dyadic filter bank [18]. The average frequency of each IMF, gives a rough criterion for choosing which IMF to include in the filtered signal. By merging the IMFs with an average frequency in the electro-mechanical range (oscillating frequency from 0.2 to 2 Hz), the high frequency components and the signal trend (given by the residual) is excluded, and a filter has been implemented.

One challenge when using the EMD, is that modes with closely spaced frequencies may be mixed together. This makes the basic version of EMD more challenging for identification of electro-mechanical modes unless special strategies are used for intermittent or closely-spaced tones as described in [19]. For high frequency filtering on the other hand, its characteristics are well suited, as it elegantly extracts high frequency components without altering the remaining signal components.

In this paper, the EMD implemented is based on the work by Deshpande [20].

E. Cluster

To solve the problem of identifying the number of modes present in a signal, and thus solve the challenge of model order selection, this paper proposes to run PA in a range of model orders. By performing PA with every model order between a lower and a higher limit, the idea is that the true modes and their shapes will remain close to constant. True modes are those that are responsible for actual linear behaviour in the system. Subsequently, the trivial modes (identified by their frequency, damping and amplitude) will change significantly. Trivial modes are those that fit the noise and nonlinear behaviour.

A lower limit of $p = 10$ and an upper limit of $p = N/2$ is chosen for the model order range to ensure a good basis for clustering. The lower limit is defined as 10 to mitigate simulations where the number of observable modes is larger than the model order.

The clustering method used in this paper is a density-based algorithm named "Density-based spatial clustering of applications with noise" (DBSCAN). This method was first proposed by Ester *et al.* [21], to make clustering more versatile. Density-based algorithms are not limited to finding spherical clusters of a predefined size. It can on the other hand, by considering the density of an area, find clusters of arbitrary shapes. It works as an unsupervised learning mechanism, labelling data in clusters and assigning the rest as noise [22].

The DBSCAN algorithm depends on two input parameters: epsilon (ϵ) and minimum cluster size (minClu). By firstly assuming that none of the input-data belongs to a cluster, DBSCAN chooses one of the unassigned objects as a starting point p. From this point all objects within a distance of ϵ is considered as a neighbour. If the point p is found to be a core point [21], it finds all objects in its area using ϵ and minClu. All these objects are then assigned to the same cluster. If p is not considered as a core object, and is not present in another cluster, it is labelled as noise. The clustering is completed once every object is either assigned to a cluster or labelled as noise.

In this paper, the input data for DBSCAN is three-dimensional. Frequency, damping and amplitude of all identified modes from all model order simulations of PA are utilised. For weighting purposes, the algorithm is altered so that only a small deviation in frequency is allowed. For amplitude and damping, some deviation is accepted in each cluster.

III. Remarks on implementation

The modes of interest in this paper, lies in the electro-mechanical range. In accordance with the Nyquist-Shannon sampling theorem [23], the sampling frequency must be at least 4 Hz to contain information of the modes at 2 Hz. In this paper the sampling frequency is set to 6 Hz, well above the minimum limit, to avoid loss of modal information. For data sampled at higher frequencies, approximately 6 Hz is achieved through downsampling. The sampling theorem applies to the high frequency noise as well. When the sampling frequency is below twice the noise frequency, information is lost and signal aliasing occurs [24]. To assure that this problem is handled, the signal is filtered for high frequency noise by using the EMD-technique, without altering the components in the electromechanical range.

For higher model orders, many of the modes found by PA have insignificant amplitudes, or very high damping ratios. These are filtered out before feeding the clustering algorithm with the modes, as they do not influence the signal dynamics. Choosing a hard limit on mode amplitude (1/30 relative to highest amplitude), and excluding modes with damping ratio above 50%, is a brute way of post-filtering the results. A more sophisticated evaluation method is presented by Zhou, Pier and Trudnowski [25]. However, the hard limit is sufficient for this method, with the purpose of removing the obvious trivial modes. The clustering algorithm is responsible for classifying the rest.

A. Proposed method

- Pre-Filtering using EMD

  - Identify signal IMFs
  - Extract IMFs in the electro-mechanical range
  - Rebuild signal without high frequency noise and signal trend
- Downsample signal to 6 Hz
- Define range of model orders to be investigated
- Do PA for all p orders in defined range
- Cluster the resulting modes

B. Steps of PA

PA_O :

- Build LPM in (5)
- Estimate **a**-coefficients using least-squares
- Find roots of characteristic polynomial in (6)
- Calculate eigenvalues from roots with (7)
- Establish equation system shown in (10)
- Solve the equation system for residual **C**

PA_F :

- Define q as $p-1$
- Build equation system in (12)
- Obtain least-square solution for **a**-coefficients
- Utilise q first equations to obtain **b**-coefficients
- Insert **a**- and **b**-coefficients into transfer function in (11)
- Calculate Laurent series expansion of transfer function with (13)
- Calculate eigenvalues from roots of denominator
- Find residual from denominator

Common for both methods :

- Calculate frequency and damping from eigenvalue
- Calculate amplitude and phase from residual
- Post-filter of insignificant modes

IV. Testing

A. Synthetic signal

First, the two methods will be demonstrated for synthetic signals. 3-dimensional plots are used to demonstrate the clustering method, as well as how the results of the Prony analysis vary with the model order.

$$\begin{aligned} y(t) = {} & 16cos(2\pi * 1.55 + 1.5\pi)e^{-0.25t} \\ & + 30cos(2\pi * 0.28 + 0.5\pi)e^{-0.04t} \\ & + 20cos(2\pi * 0.75 + 0.2\pi)e^{-0.3t} \end{aligned} \tag{14}$$

The synthetic signal tested is shown in equation (14), and contains three modes with a damping ratio (η) of 0.026, 0.023 and 0.064 respectively.

The three coloured dots in Figure 1 are actually clusters, each consisting of 55 data points obtained from PA_O, equalling the number of runs with different model orders. These results are only shown to demonstrate that the modal decomposition will be determined exactly for all model orders in the defined range, given a pure sinusoidal signal like this. Averaging each cluster, yields the modal components of equation (14) to a precision of 8 decimals. The results are similar for PA_F.

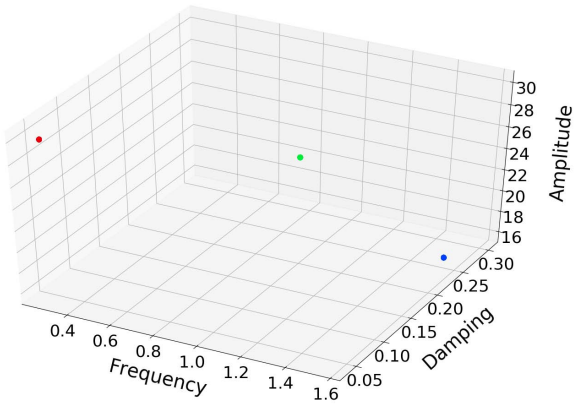

Fig. 1: Clustering of pure, synthetic signal

Introducing noise to the signal will degrade the performance of Prony, as experienced by previous authors [25]. Given the same synthetic signal, embedded in 20 dB white Gaussian noise, the performance of the EMD-filter Prony can be evaluated.

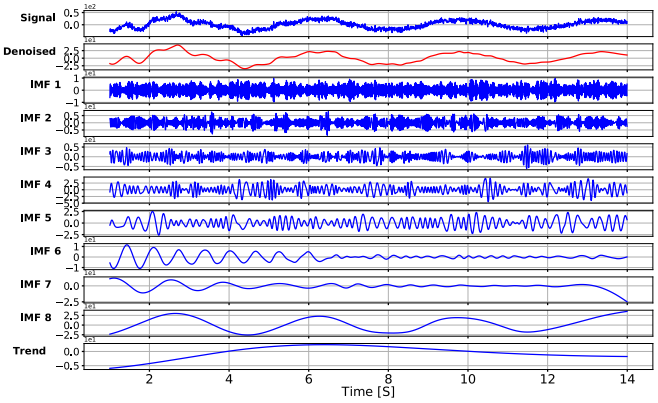

Fig. 2: Decomposing noisy signal using EMD

Summation of IMF 6 - IMF 8, yields the red, filtered signal in Figure 2. Clustering and averaging yields the modal components shown in Table I. The signal is reconstructed using only these modes in Figure 3b, which yields a signal-to-noise ratio (SNR) of approximately 43.5 dB for both methods when comparing with the EMD-filtered signal.

As seen in Table I, the frequency and damping ratio has minor deviations (less than 1/100) compared to the original signal. Amplitude and phase deviates slightly more, but are still close to original when comparing with the noise that was added to the system. When comparing the two methods, it is observed that the differences are negligible.

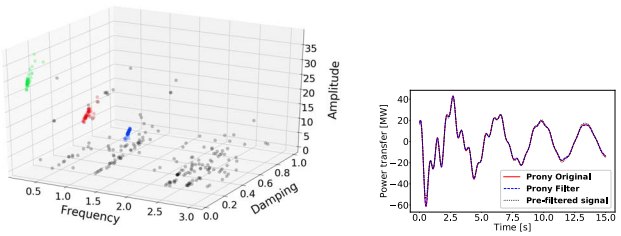

(a) Clustering of noisy, synthetic signal **(b)** Reconstruction

Fig. 3: Analysis of PMU-data

TABLE I: Consistent modes for multiple model orders

PA_O				PA_F			
Freq. [Hz]	η	**Amp.**	**Phase [rad]**	**Freq. [Hz]**	η	**Amp.**	**Phase [rad]**
0,755	0,069	21,96	$0{,}18\pi$	0,756	0,069	21,64	$0{,}18\pi$
0,278	0,026	31,42	$0{,}52\pi$	0,278	0,030	31,48	$0{,}53\pi$
1,548	0,027	16,92	$1{,}52\pi$	1,548	0,027	16,82	$1{,}52\pi$

B. Power Factory simulation

The next step is to test on measurements from a Power Factory (PF) model. The model used is the *Kundur Two Area Model* [26, p. 813] showed in Figure 4 .

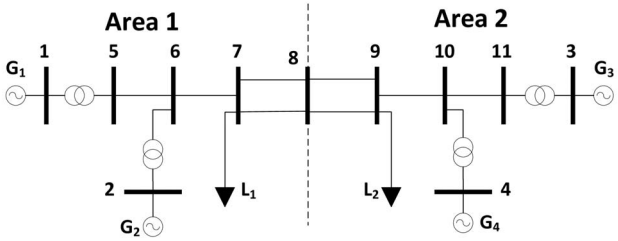

Fig. 4: Kundur Two Area System

To simulate a larger fault and create oscillations, the line between bus 6 and 7 are disconnected and reconnected 0.05 s later. Power flow measurements between bus 5 and 6, and bus 10 and 11, are then analyzed to identify modes.

Using the built-in modal analysis tool in PF, the frequency and damping of the modal components present in the system are found. It must be kept in mind that it will find all modes, and not just those that are excited by a given fault. The oscillatory modes identified by PF are:

TABLE II: Modes identified by PF

Mode	**Freq. [Hz]**	**Damp. Ratio η**
1	0,475	0,024
2	0,700	0,052
3	0,989	0,110

PF calculates the modal components present based on steady-state snapshot of the power system. In this test, variable load was added in order to better simulate the real world grid. Ambient noise was simulated as Gaussian white noise, similar to the synthetic signal. Furthermore, the ambient noise included an increase in the mean of the load 5 seconds into the time window of analysis. The result of this can be seen in Figure 5. The signal-to-noise ratio of the signal with variable load compared to the constant load signal, is approximately 10 dB for both lines. It can be noted that adding the ambient noise reduces the damping of the signal, as well as shifting the signal slightly. This continuous change in the system, makes the comparison of the modal estimation to the PF modes in Table II less trivial, as the modes change in each time-step. The assumption is then, as it was for the synthetic signal, that linear behaviour dominates the ringdown signal.

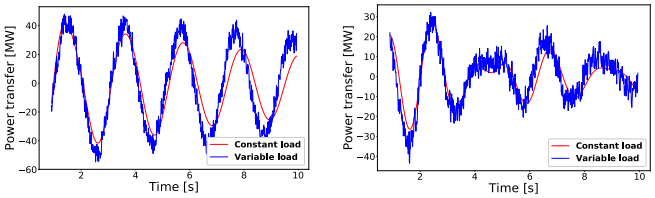

(a) Line 10-11 **(b)** Line 5-6

Fig. 5: Comparing measured signal for same fault with and without load variation

Running both PA_O and PA_F on the constant load signal, resulted in both methods identifying all three modes in the measurements from line 5-6 and line 10-11. Reconstructing and comparing to the measured signals, resulted in a signal-to-noise ratio of 50 dB and 63 dB for line 5-6 and line 10-11 respectively. The results were close to identical in PA_O and PA_F. It was also noted that for line 5-6, the 0.475 Hz mode and 0.700 Hz mode in Table II were both observable, while it was barely possible to distinguish the 0.989 Hz mode. For line 10-11, only the 0.475 Hz mode was distinguishable with a large magnitude, while the other two were small (just above 1/30 of the magnitude). With a close to 180° phase shift between the two areas, the 0.475 Hz mode is identified as a clear inter-area mode.

Figure 6a shows the ringdown signal with ambient noise. By using the EMD-method as a filter to remove high frequency components and the trend, the signal shown in Figure 6b is obtained.

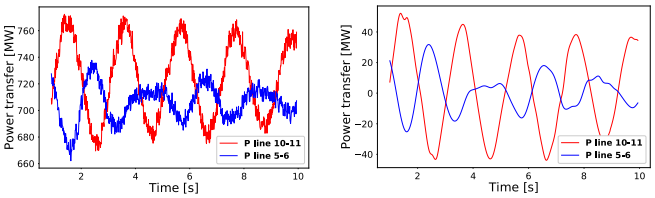

(a) Measurements before EMD-filtering **(b)** Measurements after EMD-filtering

Fig. 6: Measured signal

It can be observed that the EMD-filter removes most of the noise in the signal. Applying PA_O and PA_F combined

with clustering, gives the modal estimation shown in Table III and IV.

TABLE III: Modes identified from measurements on line 5-6

PA_O				PA_F			
Fre. [Hz]	η	**Amp.**	**Phase [rad]**	**Fre. [Hz]**	η	**Amp.**	**Phase [rad]**
0,489	0,034	20,900	$0{,}50\pi$	0,489	0,036	20,961	$0{,}53\pi$
0,710	0,048	16,153	$0{,}02\pi$	0,710	0,047	15,374	$0{,}02\pi$

TABLE IV: Mode identified from measurements on line 10-11

PA_O				PA_F			
Freq. [Hz]	η	**Amp.**	**Phase [rad]**	**Freq. [Hz]**	η	**Amp.**	**Phase [rad]**
0,486	0,014	47,946	$-0{,}52\pi$	0,486	0,015	47,999	$-0{,}52\pi$

The results are as expected not identical to Table II. The ambient noise has altered both frequency and damping, compared with results from PF as seen in Figure 5. From the measurements on the line between bus 5 and 6, only two of the modes are found. This was as expected, since these two were the most observable in the signal, while the last one barely was present. Similarly, only the most observable mode from the noise free test was found in line 10-11.

One important note is that the mode with the smallest damping ratio found by PF, still is the most critical mode with ambient noise included. With a phase-shift close to 180°, the mode oscillates between the two areas. The 0.700 Hz mode on the other hand, was barely present in Area 2 in the noise free signals and can be labelled as a local mode in Area 1. By plotting the estimated modes together with the signal after filtering, the estimation accuracy can be evaluated as seen in Figure 7.

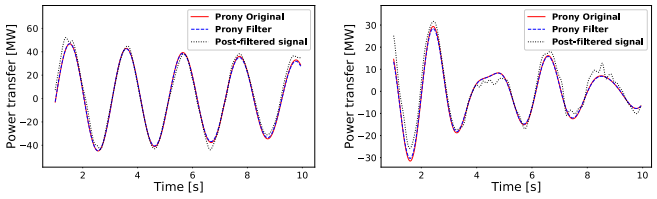

(a) Line 10-11 **(b)** Line 5-6

Fig. 7: Comparing measured signal after EMD-filtering with identified modes

The curve fit seen in Figure 7a and 7b shows that the modal components dominating the signal has been identified. PA_O and PA_F perform similarly, both estimations yielding SNR of 35 dB for Figure 7a and 22 dB for Figure 7b.

C. PMU-data

In this section, PMU-data from the nordic grid is analyzed. The PMU-measurements contain information of a production outage, with resulting oscillations in the grid. Identification of this oscillation is vital for stable operation in a smartgrid. Figure 8 shows the PMU-measurement, with the ringdown portion magnified.

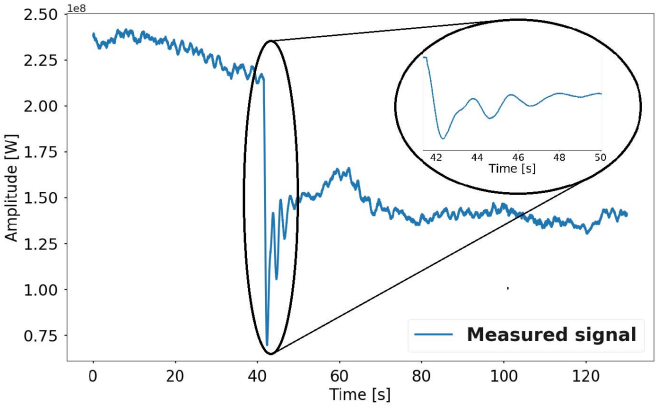

Fig. 8: PMU-data example

Even though the ringdown part of the signal is large compared to the ambient noise, the latter must be removed to avoid aliasing and improve the performance of PA. Figure 9 shows the decomposed signal. Summation of IMF 4 and IMF 5, yields the denoised signal for further analysis.

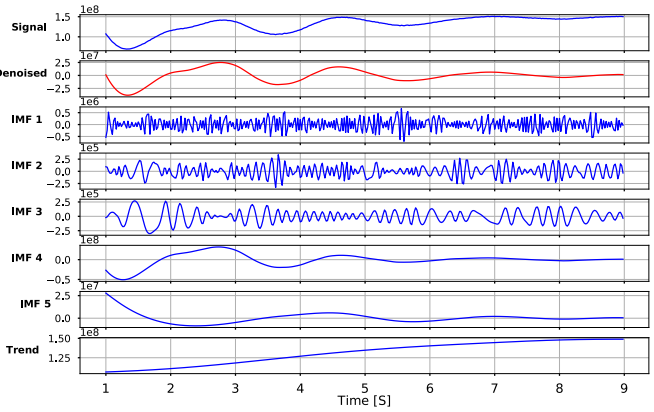

Fig. 9: Decomposing PMU-data into IMFs

Running both PA methods for 30 different model orders gives the modal plot shown in Figure 10a. The identified cluster contains data from 21 of the 30 simulations of PA_O. For PA_F 20 out of 30 simulations were connected to the identified cluster. The remaining data-points were labelled as trivial modes.

Figure 10b shows the comparison of the identified modes in Table V with the filtered PMU-measurement, where both methods had a signal-to-noise ratio of 14 dB after reconstruction. The results in Table V show small differences between the two methods. In addition, the mode identified has a damping ratio well within the limit of what is acceptable.

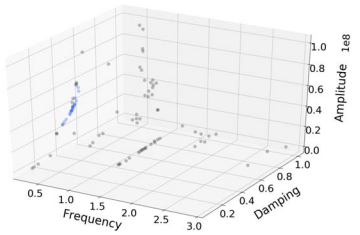

(a) Cluster identification using PA_O

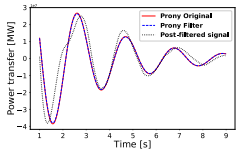

(b) Identified mode compared with original signal after EMD-filtering

Fig. 10: Analysis of PMU-data

TABLE V: Identified mode

PA_O				PA_F			
Freq. [Hz]	η	**Amp.**	**Phase [rad]**	**Freq. [Hz]**	η	**Amp.**	**Phase [rad]**
0,476	0,116	48,08	$0{,}45\pi$	0,477	0,117	47,91	$0{,}44\pi$

D. Computational burden

From Table VI it can be observed that the most demanding routine is PA_F, spending close to or more than twice the time of PA_O in all tests. The EMD spends in general less time than PA, although it must be kept in mind that the Prony method's are run for 30 or more different model orders. The clustering algorithm spends a negligible amount of time. These tests were run using Intel Core i7 8650U.

TABLE VI: Computation time in seconds

	Synthetic signal	**PF**	**PMU**
Time window	15	12	10
EMD filter	0,235	0,193	0,089
PA_O	0,514	0,255	0,117
PA_F	0,903	0,369	0,292
Clustering	0,003	0,002	0,001

V. Conclusion

The intuition of Prony Analysis, along with it's main drawbacks, have been addressed in this paper. Pre-filtering of signal noise and trend is elegantly performed by the EMD technique, and improves performance of PA in noisy conditions. Performing PA for multiple model orders, indicates the consistency of true modes, and fluctuations of trivial modes. This phenomena is exploited by the clustering method, enabling correct identification of true modal components. This method is versatile, as demonstrated by testing for both Prony methods. Improvements to PA, like recursive implementation for real-time observation and control, can be incorporated into the clustering method. Comparing PA_O and PA_F reveals only small differences in performance, except for the extra computation time required in PA_F.

Acknowledgment

The authors would like to thank Prof. Kjetil Uhlen of NTNU for providing PMU-data and Dinh Thuc Duong of NTNU for sharing his experience with PA in the power system.

References

[1] G. Prony, "Essai experimental–,-," *J. de l'Ecole Polytechnique*, 1795.
[2] J. Hauer, "Initial results in prony analysis of power system response signals," *IEEE Transactions on Power Systems*, vol. 5, no. 1, 1990.
[3] Z. Huang, N. Zhou, F. K. Tuffner, Y. Chen, D. J. Trudnowski, R. Diao, J. C. Fuller, W. A. Mittelstadt, J. F. Hauer, and J. E. Dagle, "Mango – modal analysis for grid operation: A method for damping improvement through operating point adjustment," October 2010.
[4] A. R. Borden, B. C. Lesieutre, and J. Gronquist, "Power system modal analysis tool developed for industry use," in *North American Power Symposium (NAPS), 2013*, pp. 1–6, IEEE, 2013.
[5] W. J. S. I. Subcommittee, "Oscillation detection and analysis applications in wecc." https://www.wecc.biz/Reliability/WECC%20JSIS%20Oscillation%20Detection%20and%20Analysis%20Applications%20-%202013-06-12-APPROVED.pdf, Nov. 2012.
[6] A. R. Borden and B. C. Lesieutre, "Variable projection method for power system modal identification," *Power Systems, IEEE Transactions on*, vol. 29, pp. 2613–2620, November 2014.
[7] R. Barbosa, J. Tenreiro Machado, and M. Silva, "Time domain design of fractional differintegrators using least-squares," *Signal Processing*, vol. 86, pp. 2567–2581, October 2006.
[8] N. Zhou, Z. Huang, F. Tuffner, S. Jin, J. Lin, and M. Hauer, "Final project report oscillation detection and analysis," *CIEE report.[online]. Available: https:// uc-ciee.org/ downloads/ ODA_Final_ Report.pdf*, 2010.
[9] T. H. Park, "Linear time-invariant systems," in *Introduction To Digital Signal Processing*, pp. 122–144, World Scientific Publishing Co. Pte. Ltd., 2010.
[10] D. Lynch, "Numerical partial differential equations for environmental scientists and engineers," ch. 2.1, Springer US, April 2005.
[11] G. Strang, "Introduction to linear algebra," 2009.
[12] B. Lathi, *Signal processing and linear systems*, ch. 11. Carmichael, Calif: Berkeley Cambridge Press, 1998.
[13] J. Hauer, "Application of prony analysis to the determination of modal content and equivalent models for measured power system response," *IEEE Transactions on Power Systems*, vol. 6, no. 3, 1991.
[14] J. D. Broesch, "Digital signal processing demystified," 2000.
[15] R. Kumaresan and Y. Feng, "Fir prefiltering improves prony's method," *IEEE Transactions on Signal Processing*, vol. 39, no. 3, pp. 736–741, 1991.
[16] J. Sanchez-Gasca and D. Trudnowski, "Identification of electromechanical modes in power systems," *IEEE Task Force Report, Special Publication TP462*, 2012.
[17] G. Rilling, P. Flandrin, P. Goncalves, *et al.*, "On empirical mode decomposition and its algorithms," in *IEEE-EURASIP workshop on nonlinear signal and image processing*, vol. 3, pp. 8–11, NSIP-03, Grado (I), 2003.
[18] P. Flandrin, G. Rilling, and P. Goncalves, "Empirical mode decomposition as a filter bank," *IEEE signal processing letters*, vol. 11, no. 2, pp. 112–114, 2004.
[19] O. B. Fosso and M. Molinas, "Method for mode mixing separation in empirical mode decomposition," September 2017.
[20] J. Deshpande, "Pyhht tutorials." http://pyhht.readthedocs.io/en/latest/tutorials.html, 2015.
[21] M. Ester, H.-P. Kriegel, J. Sander, X. Xu, *et al.*, "A density-based algorithm for discovering clusters in large spatial databases with noise.," in *Kdd*, vol. 96, pp. 226–231, 1996.
[22] J. Erman, M. Arlitt, and A. Mahanti, "Traffic classification using clustering algorithms," in *Proceedings of the 2006 SIGCOMM workshop on Mining network data*, pp. 281–286, ACM, 2006.
[23] C. E. Shannon, "Communication in the presence of noise," *Proceedings of the IRE*, vol. 37, no. 1, pp. 10–21, 1949.
[24] G. D'Antona, "Digital signal processing for measurement systems : Theory and applications," 2006.
[25] J. W. Ning Zhou, D. Pierre, and D. Trudnowski, "A stepwise regression method for estimating dominant electromechanical modes," *Power Systems, IEEE Transactions on*, vol. 27, pp. 1051–1059, May 2012.
[26] P. Kundur, "Power system stability and control," 1994.